Supplemental Data

Figure S1, Related to Figure 1

A

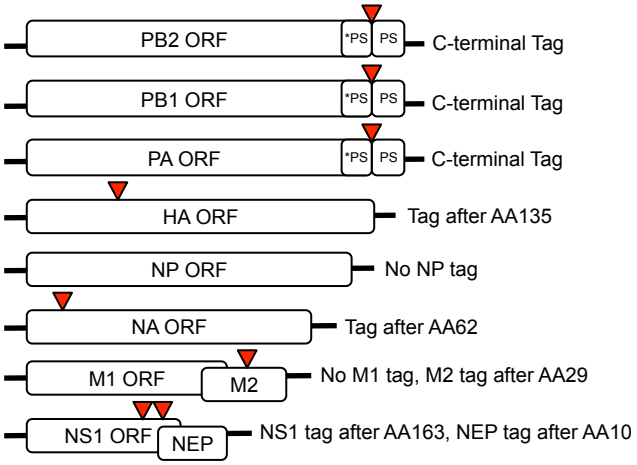

B

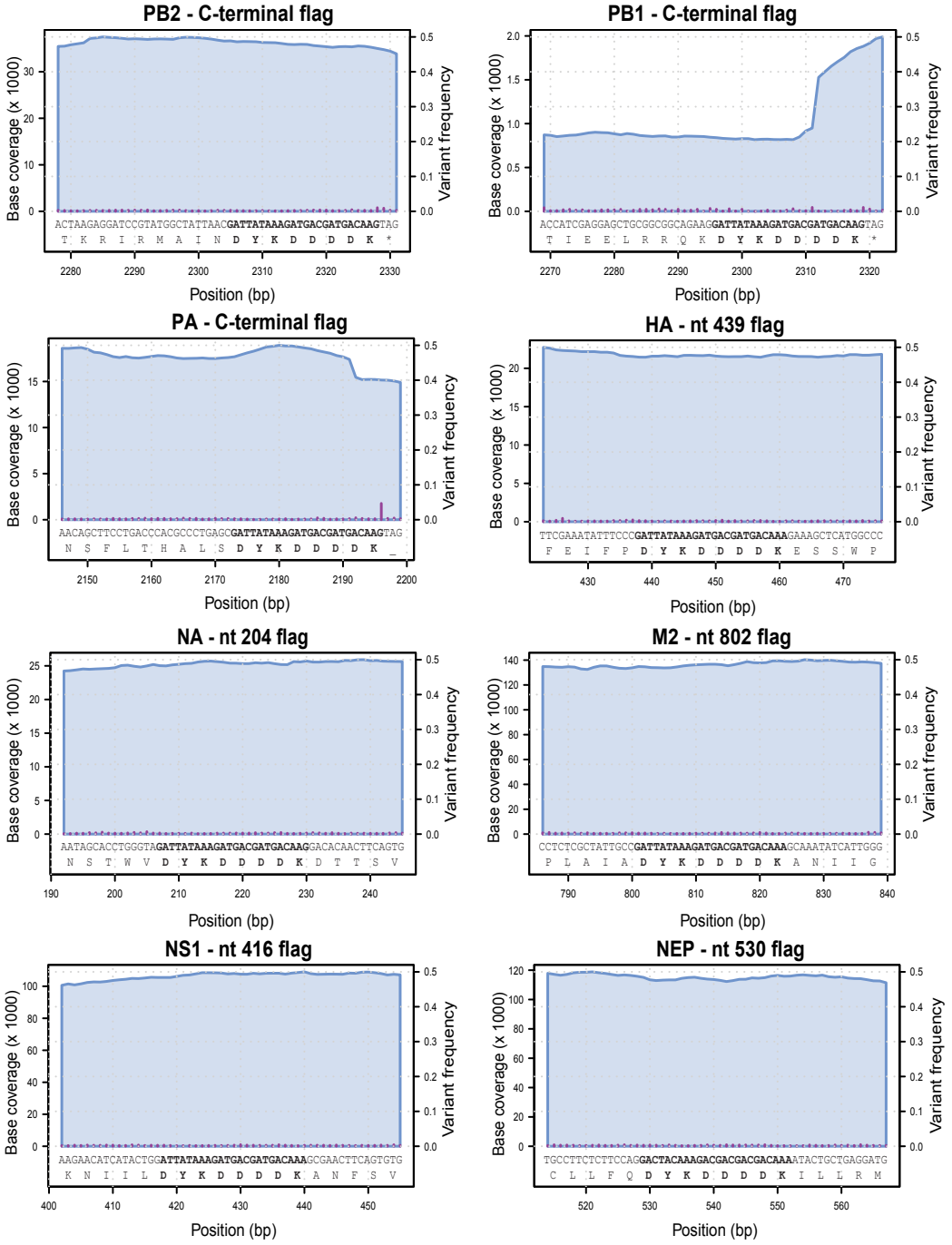

C

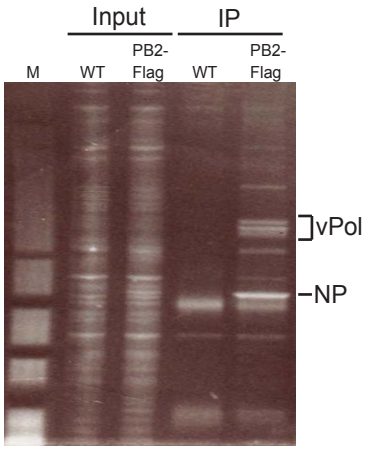

Figure S2, Related to Figure 2

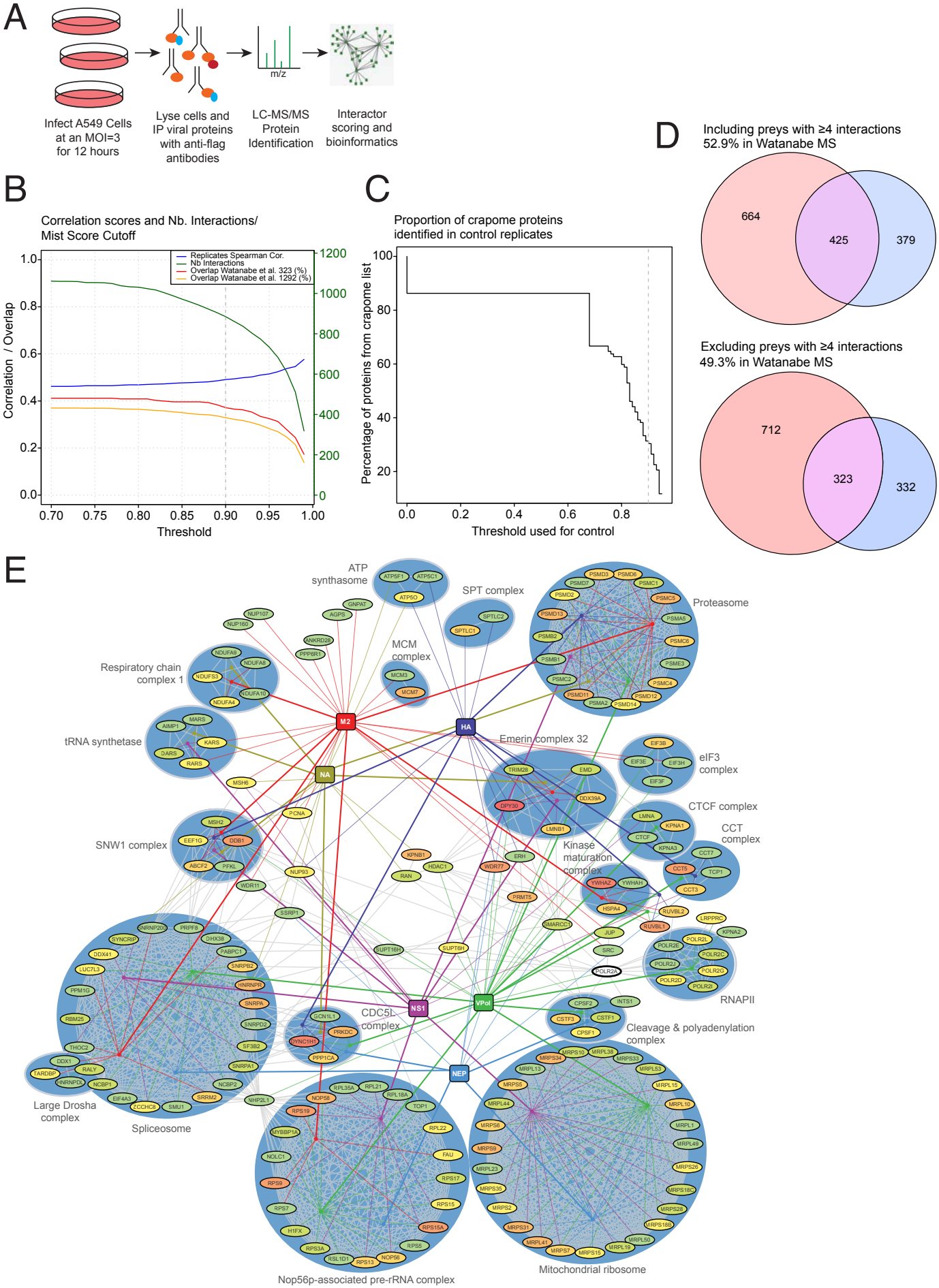

Figure S3, Related to Figure 2

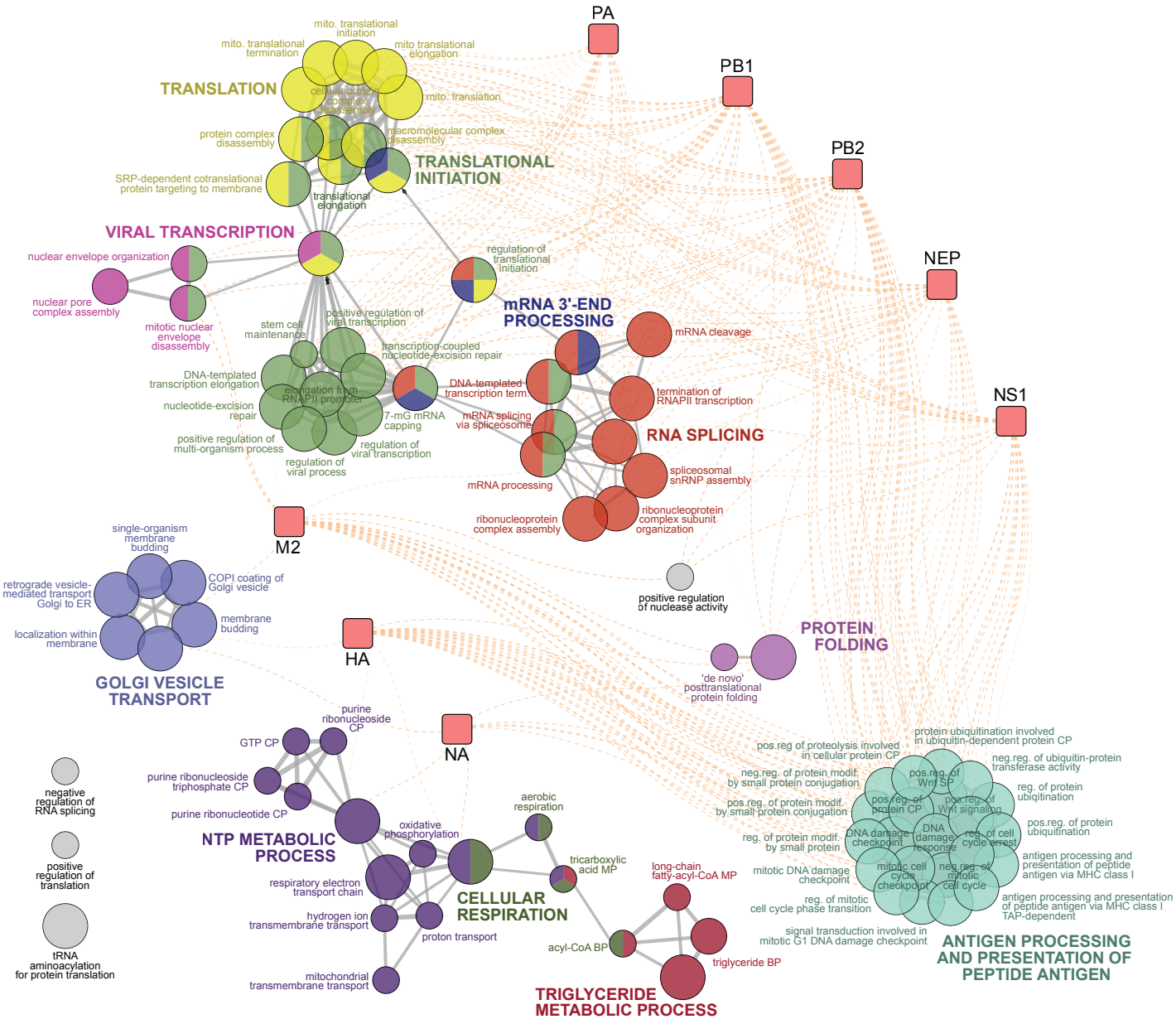

Figure S4, Related to Figure 3

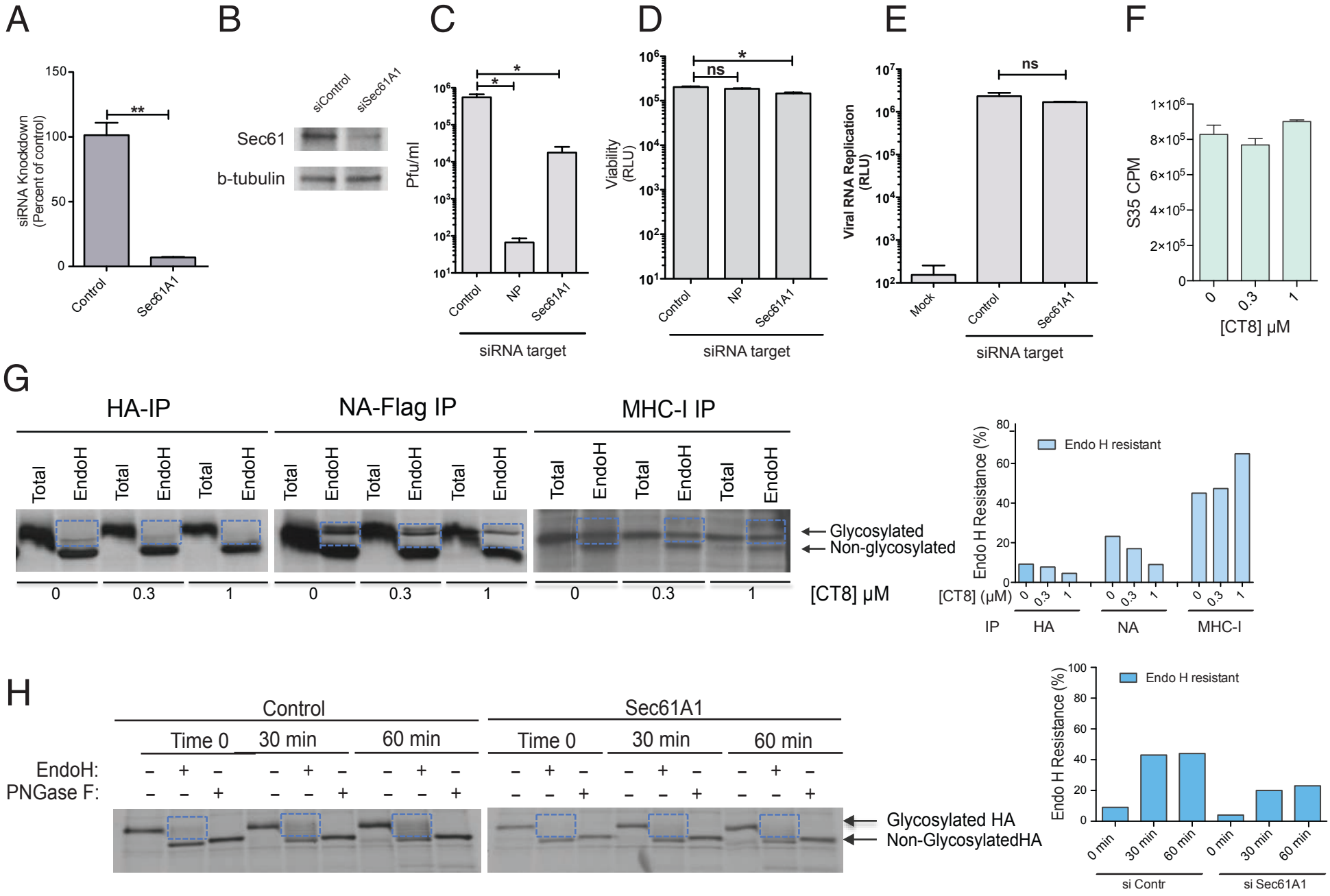

Figure S5, Related to Figure 4

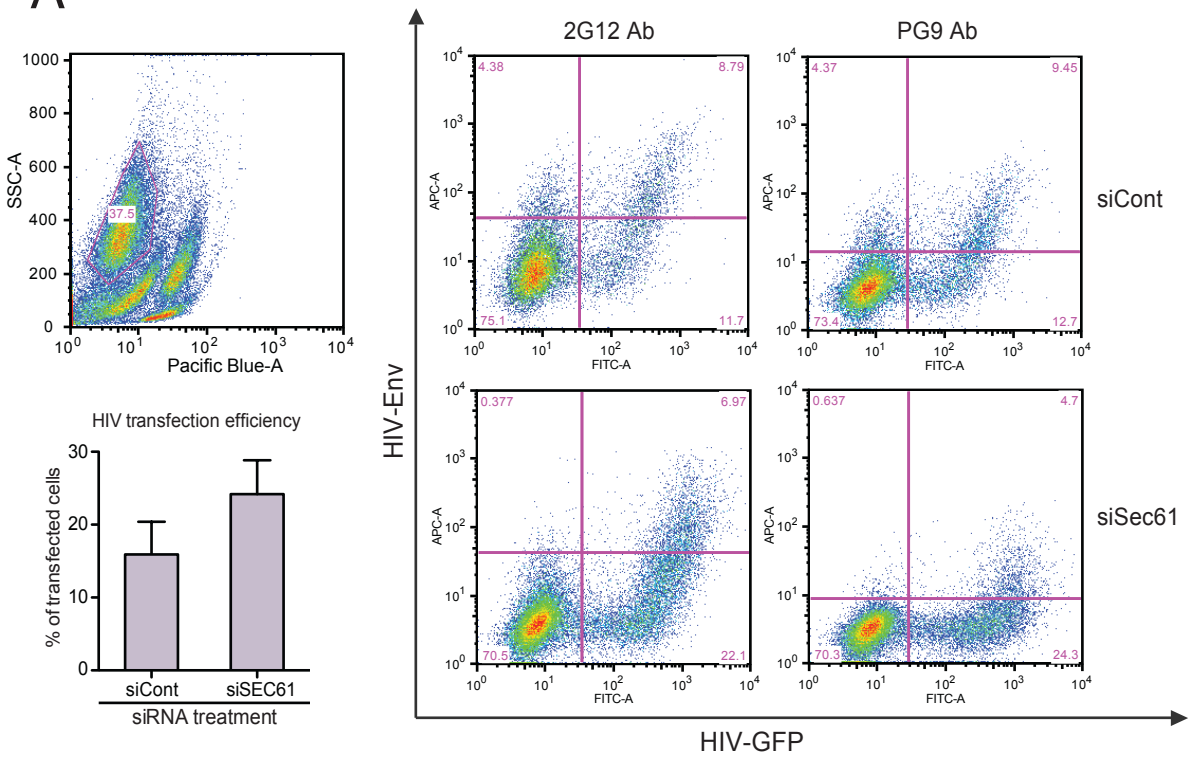

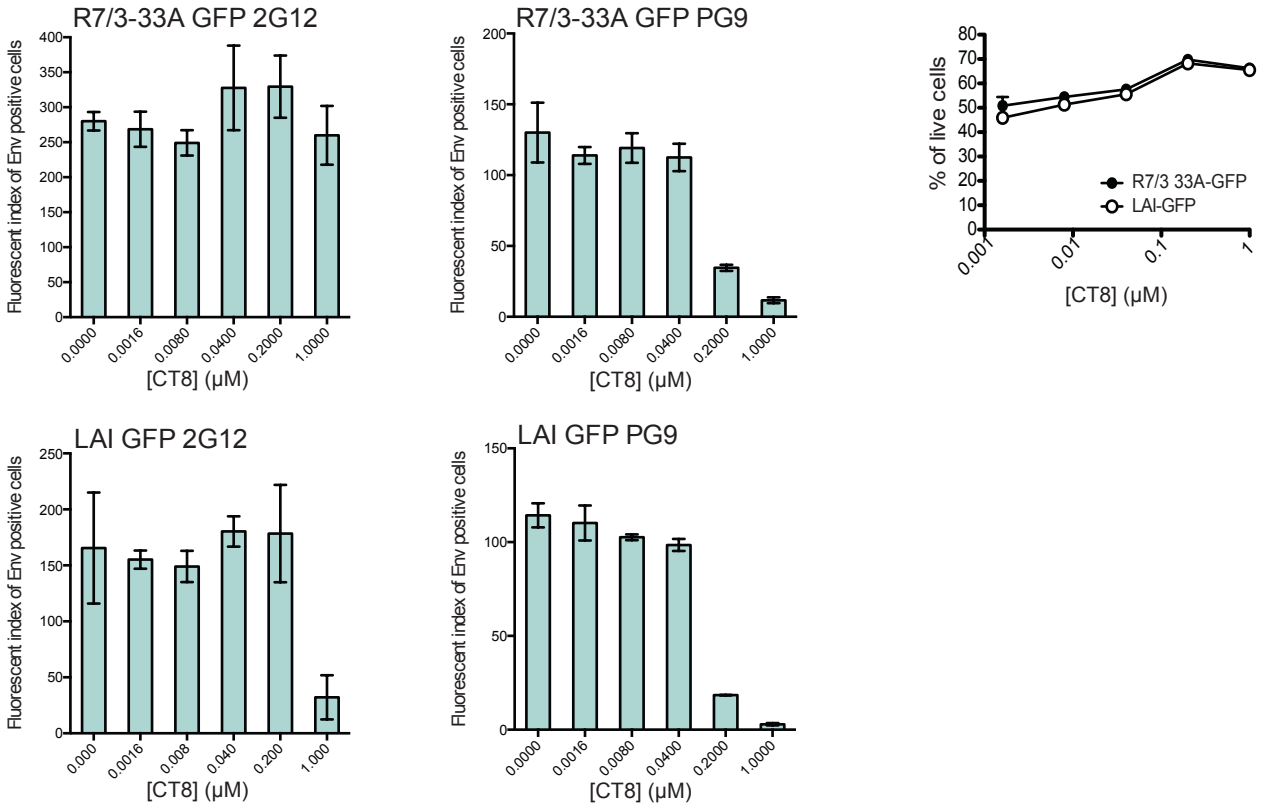

Supplemental Figure Legends

Figure S1. Tagged Influenza viruses.

This figure is linked to Figure 1.

(A) Schematic map of the compendium of tagged viruses. The ORF of each segment is indicated with the Flag tag insertion site (red triangle). **(B)** Sequencing of RNA from tagged viruses passaged and propagated at least two times reveals that the sequence encoding the Flag epitope is retained throughout generations. The PB1 has lower read coverage compared to the other viruses but still retain higher than 99.5% identity of the tag similarly to the rest of the Flag-virus. **(C)** Cells were infected with WT or PB2-Flag virus. After affinity purification proteins were resolved and stained with SYPRO Ruby.

Figure S2. Degree of overlap between significant interactors and external datasets.

This figure is linked to Figure 2 and Tables S1-S4 with the raw and processed AP-ms datasets.

(A) Schematic of AP-ms. **(B)** Relationship between MiST score threshold and 1) the number of interactions identified (scale on right); 2) the spearman correlation between replicate experiments (scale on left); and 3) the fraction of interactors identified in (Watanabe et al., 2014) accounted for before (1292 proteins) and after applying siRNA filtering (323 proteins; scale on left). The MiST score cutoff used in this study is indicated (dashed grey line). **(C)** Fraction of known contaminants (Crapome database, see Supplemental Experimental Procedures) identified in replicate control experiments at different MiST score thresholds. The MiST score cutoff used in this study is indicated (dashed grey line). **(D)** Venn Diagram representing the overlap between interactors

identified in this study (blue circle, MiST threshold of 0.9) and lists of proteins identified in (Watanabe et al., 2014). Two diagrams correspond to the two datasets analyzed with the inclusion (our dataset) of preys with ≥ 4 interactions (top diagram) and excluding preys with ≥ 4 interactions (lower diagram and Table S4). The rationale of filtering out host proteins that interact with 4 or more viral proteins was an attempt to remove putative contaminants. Since vPOL complex is formed by 3 subunits, we utilize 4 or more as a threshold. This analysis is not unbiased and we provide this additionally filtered datasets as Table S4. **(E)** Proteomic interaction network of influenza virus proteins. Interactions between influenza virus proteins and human protein complexes from the Comprehensive Resource of Mammalian Protein Complexes (CORUM). Viral nodes (proteins) and edges (interactions) are colored according to the viral protein. Interactions involving the PB1, PB2 and PA viral polymerase complex subunits were grouped (VPol; green). Human proteins are colored by the number of viral protein interactions. Edges connecting complexed proteins are shown in grey. The network only includes interactions between a virus protein and host complex if the viral protein was found to interact with two or more proteins in the complex.

Figure S3. Gene ontology analysis of host-viral protein interactions.

This figure is linked to Figure 2

ClueGo biological process network of viral protein interactions identified by Mass Spectrometry at a score threshold of ≥0.6. Nodes are colored according to major biological process groups. Orange lines link each viral protein with GO terms that are

significantly enriched among its interacting proteins. Grey lines reflect GO term relationships.

Figure S4. Sec61A1 depletion or chemical inhibition suppresses influenza HA and NA biogenesis and inhibits viral growth.

This figure is linked to Figure 3

A549 cells were treated with a non-targeting control siRNA, and a Sec61A1 siRNA for 48 hours. **(A)** Sec61A RNA levels were quantified via RT-PCR Taqman assay. **(B)** Sec61A1 and b-tubulin (loading control) proteins were detected via western blot. Representative of two experiments is shown. **(C-D)** A549 cells were treated with the control, Sec61A1 and Influenza NP siRNAs. Effects on release of virus **(C)** and cellular viability **(D)** are indicated. **(E)** A549 cells treated with control or Sec61A1 siRNAs were infected with a luciferase reporter influenza PR8 virus for seven hours in the absence of trypsin. For all panels, *$p \leq 0.05$, **$p \leq 0.001$, ns=not significant. **(F)** 35-S Methionine incorporation levels were measured by S35 CPM in control and treated with CT8 A549 cells. **(G)** A549 cells were infected with Flag-NA at an MOI=1 and treated with the substrate specific Sec61 inhibitor CT8 at the indicated concentrations. Five hours post-infection, cells were amino acid starved for 30 minutes, pulsed with 35-S for 30 min and chased with cold amino acids for 60 minutes. Post-nuclear lysates were then split and subjected to Immunoprecipitation with antibodies that recognize HA trimers (6F12), Flag-NA, and MHC-I, followed by splitting each sample in two parts and treating one with PBS and another with EndoH. HA, NA and MHC-I amounts were detected by autoradiography and HA glycosylation levels were quantified by single densitometry measurements of each

sample. Endo H resistance amounts (blue boxes) were calculated relative to the total protein amounts. **(H)** A549 cells were treated with control or Sec61A1 siRNAs. Five hours post-infection, cells were processed as in (G) and chased with cold amino acids for the indicated times. Total HA was immunoprecipitated and subjected to buffer alone, EndoH, or PNGase treatment. The amounts of glycosylated HA were analyzed by autoradiography and quantified based on the relative intensity measurements of samples resistant to Endo H treatment (single densitometry measurements as in (G)).

Figure S5. CT8 inhibits HIV replication.

This figure is linked to Figure 4.

(A) Gating strategy. HEK 293T treated with SEC61 siRNA or control siRNA were transfected with full-length HIV-1 genomic constructs (R7/3 GFP and LAI GFP). 24 hours post transfection cells were stained for gp120 using 2G12 antibody-Alexa647 and PG9 antibody-Alexa647. Dead cells were excluded from the analysis using LIVE/DEAD Aqua Dead Cell Stain. Histogram shows that silencing of SEC61 does not impact efficiency of transfection (n=3). **(B)** HEK 293T transfected with full-length HIV-1 genomic constructs (R7/3 GFP and LAI GFP), were treated with increasing amounts of CT8. Momomeric gp120 expression was determined by staining with 2G12 antibody and trimeric gp120 was determined by PG9 staining followed by Flow Cytometry analysis (n=3). **(C)** Cell viability after CT8 treatment from (B) was determined by Cell titer Glow (Promega).

Supplemental Tables

Table S1: Processed mass spec data: Identified viral peptides co-immunoprecipitated by each Flag-tagged viral bait. Related to Figure 2.

Table S2: List of Gene Ontology terms. Related to Figure 2 and Figure S3.

Table S3: Raw mass spec data: Identified viral peptides co-immunoprecipitated by each Flag-tagged viral bait. Related to Figure 2.

Table S4: Processed mass spec data: Host protein identified ≥ 4 prey relative to Figure S2D. Related to Figure 2.

Supplemental Experimental Procedures

Identification of protein-protein interactions by AP/MS

We employed an AP-ms strategy previously described (Miller et al., 2015). AP-MS experiments for each Flag-tagged viral protein (baits) were performed in two independent experiments, and the MiST scoring system (Jager et al., 2012) was used to rank physical interactors (preys). MiST processing was done on the complete data matrix of intensity scores (Mascott peak area) derived from bait and control experiments (Wild-type, GFP, uninfected), ignoring the computation of specificity between baits, selecting the 'HIV Trained' running mode as recommended in the documentation, and disabling the filtering of singletons. Bait-prey pairs with a MiST score >0.9 and exceeding the MiST scores of the prey in all control conditions by at least 10% were selected as significantly enriched. Missing values in the data matrix were attributed an intensity score of 0. We additionally removed common contaminants that were detected in at least half of the experiments present in the Crapome reference database (Mellacheruvu et al., 2013), as well as any proteins with identifiers marked as invalid in UniProt release 2015_01. (See Supplemental Experimental Procedures for statistical analysis).

Network analysis

Human:viral protein interaction networks were plotted in CytoScape (version 3.1) (Smoot et al., 2011) using the 'spring' algorithm (no weighting). The Biological Process network was generated by analyzing all unique preys identified in the MiST analysis using the

CytoScape plugin 'ClueGO' (version 2.1.5) (Bindea et al., 2009) and the 'biological process' GO database (version 25/01/2015, all evidences without IEA). The following parameters were set in the analysis: Use GO term fusion: True; Show only Pathways with pV<: 0.05; GO Terms Restriction (GO Tree Levels): Min Level 2, Max Level 10; GO Terms Restriction (#/% Genes): Min # Genes 3, Min % Genes 10; GO Terms connection restriction (Kappa Score): 0.25; Use GO Term Grouping: True; Leading Group Term Based on: Highest Significance, Kappa Score; Initial Group Size: 2; % for group Merge: 50. Bait sample nodes and their relation (links) to GO nodes were subsequently added using a custom Jython script based on the number of significant prey interactions with each GO node. A minimum number of 5 interacting preys were required for a link to be drawn.

KEGG and GO enrichment analysis

The set of preys interacting with each viral protein were analyzed for significant KEGG category enrichment (p-Value < 0.01, g:SCS method for multiple testing correction, and 'Best per parent' hierarchical filtering), using 'G:profiler' (Reimand et al., 2011). The tabular results were further processed using a custom R-script (available on request) to generate figures with three matrix panels indicating the overlap between preys and enriched KEGG categories, prey-bait interactions, and enriched KEGG categories for each bait. The order of rows and columns were determined by a hierarchical clustering algorithm that groups baits and categories with similar enrichment patterns (complete clustering based on Spearman correlation distance). GO analysis was performed analogously, but using the Bioconductor 'topGO' package (Gentleman et al., 2004) and

the 'org.Hs.eg.db' annotation database. Significant enrichment of GO ‘biological process’, ‘molecular function’ and ‘cellular component’ terms was determined using the 'elim' algorithm and 'fisher exact' statistic test. The top 10 significant terms ($P < 0.01$) were selected for each bait and plotted as a graphical summary of the scores (-10 log10 (P-Value)) for each enriched term (columns) across all baits (rows). Baits were grouped by hierarchical clustering (complete, spearman correlation) on the score matrix merged for all GO categories (BP, MF, CC).

Comparison with previous interaction datasets

To compare our interactome analysis with previous studies, we looked at our high-confidence set of interactors and a list of cellular proteins interacting with transiently transfected IAV genes from multiple studies (Bradel-Tretheway et al., 2011; Jorba et al., 2008; Lin et al., 2012; Mayer et al., 2007; Navratil et al., 2009; Shaw et al., 2008; Tafforeau et al., 2011) reviewed in reference (Watanabe et al., 2010). We also analyzed the overlap of interactions identified in a transfection-based interaction study (Watanabe et al., 2014) and in our study (Tables S1-S4 and Figure S2D). Our analysis suggests that the cellular contexts analyzed during infection increase our ability to discover novel interactions dependent on viral protein complex formation (i.e. viral RNPs) and between viral and host proteins induced as a result of the infection.

Mathematical Modeling of distance relatedness between interactomes

We used the large-scale interactome derived in reference (Menche et al., 2015) of all known human gene interactions to determine the relatedness of pairs of proteins

containing one influenza protein and one HIV protein, inferred from HIV infected Jurkat cells. For each pair of proteins, we first loaded a list of known genes with which each protein interacts. For influenza proteins, the human proteins they interact with were taken from our work, for HIV they were taken from reference (Jager et al., 2012). We then calculated s_{AB} the network-based separation of the protein pair, using the formula

$$s_{AB} = d_{AB} + \frac{(d_{AA}+d_{BB})}{2}.$$

The s_{AB} value is the average shortest distance between A-B gene pairs (Menche et al., 2015). In the above A represents the list of human genes with which a given influenza protein in known to interact and B is a list of genes with which a given HIV protein is known to interact. It is calculated by measuring how far each influenza gene's interactors are the nearest HIV gene's interactors in the interactome, as well as how far each HIV gene is from the nearest influenza gene, and averaging these measurements. The measurement for a gene will be 0 if it is in the data sets of both proteins. The s_{AB} value is the average shortest distance within the influenza protein. It is calculated by measuring how far each influenza gene is from the nearest influenza gene that is not itself and averaging these measurements. The s_{AB} value is the average shortest distance within the HIV protein.

A small, negative s_{AB} value means that a protein pair is closely related, whereas a larger or positive s_{AB} value means that a protein pair is not closely related. We ranked the Influenza/HIV protein pairs by s_{AB} and found that the most closely related pairs were as follows:

Rank	**Influenza Protein**	**HIV Protein**	**Relatedness** (s_{AB})
1	NA	GP160	-0.24
2	NA	VPU	-0.19
3	M2	VPR	-0.18
4	HA	GP160	-0.18
5	M2	GP160	-0.17

For each of these five pairs, we created a list of genes that were either 0 or 1 node away from any gene in the other protein dataset. We then generated a gene ontology report for each list and analyzed the five reports to see which categories showed up most frequently and with the lowest *p*-value. Categories which were either (a) related to both protein localization and the endoplasmic reticulum or (b) related to the signal-recognition particle (SRP) showed up in all the reports and had low *p*-values.

Gene Ontology Category	**# of Reports w/ Category**	***p*-Value**
SRP-dependent cotranslational protein targeting to membrane	5	$3.5 * 10^{-58}$

protein localization to endoplasmic reticulum	5	$1.2 * 10^{-57}$
establishment of protein localization to endoplasmic reticulum	5	$1.6 * 10^{-56}$

Animal infections

BALB/c mice were purchased from the Jackson Laboratory (Bar Harbor, ME). Mice were anesthetized with ketamine/xylazine and infected with the indicated doses of viruses. Body weight was monitored over the course of infection and 80% initial body weight was designated as the humane endpoint. No randomization or blinding. Sample size n=5 per data point. All experiments involving animals were performed in accordance with the Mount Sinai School of Medicine Institution of Animal Care and Use Committee.

siRNA treatment

To test the effect Sec61A1 silencing, cells were first transfected with Sec61A1 siRNAs (Life Technologies s26723 and s26722) or control siRNA using RNAiMax Transfection Reagent (Life Technologies) as per the manufacturers instructions. Sec61A1 RNA levels were determined via RT-PCR using Taqman primer/probe sets to detect Sec61A1 and GAPDH RNA (Applied Biosystems: Hs01037684_m1 and Hs02758991_g1), as well as the 18S control primer/probe set (Applied Biosystems 4319413E). For influenza studies, A549 cells were silenced for 48 hours before infection. To test HIV-1 Env surface expression, HEK 293T cells were transfected with Sec61A1 siRNA (Life Technologies s26723) and control in a 6 wells. 24 hours after siRNA transfection, cells were split 1:3 and re-plated. After an additional 24 hours, cells were transfected with 3 μg/well HIV-1

expressing vector R7.3 33A EGFP (Chakrabarti et al., 2002; Lue et al., 2002) (a kind gift from Cecilia Cheng-Mayer, Aaron Diamond AIDS Research Center, The Rockefeller University) containing the EGFP reporter in the *nef* position using 3μg/ml polyethilenimine from Polysciences (Boussif et al., 1995). Cells were then analyzed for Env surface expression by flow cytometry. Infectivity of the viral supernatants was measured by infecting TZM-bl reporter cell-line and quantifying β-Galactosidase activity 48 hours later.

CT8 treatment of Influenza, HIV and DENV

Influenza: A549 cells were infected for 1hr at 37C at an MOI=0.5, followed by media replacement with post-infection media (Opti-MEM+BSA+Pen/Strep, Invitrogen) containing 1μg/mL TPCK trypsin and the indicated concentrations of CT8. 24 hours post-infection, viral titer was assessed via plaque assay and cellular viability as assayed using CellTiter-Glo® Luminescent Cell Viability Assay (Promega).

HIV: To assess the effect of Sec61 targeting drug CT8 on HIV-1 viral replication we used CD4/CXCR4/CCR5+ T-Lymphoblastoid Cell Line A3R5.7. $3*10^5$ cells were treated with the indicated concentrations of CT8 and infected with the following HIV-1 lab adapted viral strains R7.3 33A EGFP, NL4.3 and LAI using an MOI of about 0.002. After 24 hours cell were washed 3 times, and thereafter culture supernatants were collected every 2 days for quantification. CT8 treatment was kept constant throughout the duration of the experiment. Infections were carried out in triplicates. Virus quantification was performed using TZM-bl reporter cell-line as described above. Drug toxicity was assessed using CellTiter-Glo® Luminescent Cell Viability Assay (Promega). To test the

effect of Sec61 chemical inhibitor CT8 on HIV-Env surface expression HEK293T cells plated in 24 well plates were transfected with plasmids encoding HIV-1 R7.3 33A GFP or LAI GFP. Five hours after transfection cells were treated with increasing concentrations of CT8, (0.0016, 0.008, 0.04, 0.2, 1μM or DMSO). 24 hours after transfection HIV-1 Env surface expression was measured by flow cytometry. HIV-1 replication assays were performed as described above.

DENV: Human DCs were obtained as described in the Supplemental Experimental Procedures, and at day 5 of culture, samples of 0.5 x 10^6 cells were plated in a 12 wells plate in 500 μl of DC-medium were treated with the indicated concentrations of CT8 and infected for 45 min at 37°C with the indicated MOI of virus (diluted in DC media) or with DC medium (mock group) in a total volume of 500μl. After the adsorption period, DC medium supplemented with 10% FBS was added up to a final volume of 1ml, and cells were incubated for the appropriate time at 37°C.

Bortezomib, Spliceostatin, Castanospermine, Oligomycin A and UK5099 Treatment

A549 cells were treated with the inhibitors Bortezomib (Selleckchem, S1013), Spliceostatin (a generous gift from Kazunori Koide, Department of Chemistry, University of Pittsburgh), Castanospermine (Calbiochem, 218775), Oligomycin A (Sigma, 75351) and UK5099 (Sigma, PZ0160) in DMEM media for 1hr, media was removed and replaced with Luciferase virus/0.3% BSA mixture at an MOI=0.05 and incubated at 37°C/5% CO2 for 1 hour. Mixture was removed and replaced with complete DMEM media containing 0.2ug/mL TPCK Trypsin. Cells were collected at 12, 24, 36 and 48

hours after infection, lysed and prepared for Luciferase read out using the Promega Renilla Luciferase Assay kit as described in manufacture protocol.

HA Immunoprecipitation and Co-IP

To IP HA monomers and trimers, A549 cells infected for 7 hours were lysed in 0.2% NP40, 50 mM Tris–HCl pH 7.5, 200 mM NaCl, 1 mM EDTA. Post-nuclear lysates were split in half and either incubated with the HA head antibody PY102 (Moran et al., 1984) to IP total HA, or the stalk specific 6F12 antibody (Tan et al., 2012) to IP trimers. Anti-mouse IgG Dynabeads (Life Technologies) were used to bind the antibodies and purify HA. Washed beads were incubated with 2x Laemmli buffer and proteins were resolved via SDS-PAGE. PY102 was used for western blot analysis. For Co-IP, the human lung epithelial A549 cells were infected with HA-Flag containing IAV PR8. HA-Flag enriched fractions were obtained by subjecting crude ER extract (see subcellular fractionation in Supplemental Experimental Procedures) to immunoprecipitation using Anti-Flag M2 affinity agarose gel (Sigma).

Biotinylation and isolation of cell surface proteins

$2*10^7$ HEK293T WT and Mut cells were pre-incubated with indicated concentrations of CT8 for 2 hours followed by infection with PR8 Flag-HA virus for 10 hours at an MOI=5. Cells were washed with PBS and incubated with Sulfo-NHS-SS-Biotin for 30 min at 4° C for labeling surface proteins. After quenching labeling reaction with the Quenching Solution cells were lysed in Lysis Buffer containing protease and phosphatase inhibitors (5 cycles 30'ON/OFF with Diagenode Bioruptor). Samples were then

incubated 30 min on ice followed by centrifugation (10,000 × g for 2 minutes at 4° C). Collected supernatant fractions were subjected to affinity purification using NeutrAvidin Agarose Resin that captures biotinated proteins. Beads were washed with Wash Buffer containing protease and phosphatase inhibitors and eluted with SDS-PAGE Sample Buffer containing 50mM DTT according to the manufacture protocol (Pierce Cell Surface Protein Isolation Kit, 89881).

Immunoblotting

Samples were reduced and denatured in Laemmli buffer (95°C, 5 min) and proteins were resolved via SDS-PAGE followed by transferring to PVDF membranes (Bio-Rad). The commercially available polyclonal anti-Human Sec61A1 (LifeSpan BioSciences) and the monoclonal anti-Flag M2-Peroxidase (HRP) antibodies (Sigma) were used. The anti-Human Sec61B as previously described (Wiertz et al., 1996) and MHC-I antibodies were a gift of Domenico Tortorella (MSSM). Anti-HA antibodies PY102, 6F12 as well as the anti-M1/M2 antibodies were generated by the Center for Therapeutic Antibody Discovery at Mount Sinai. The polyclonal anti-Human Calnexin was purchased from Bethyl (A303-694A) and the monoclonal b-Tubulin antibody was purchased from Cell Signaling (2128). The antibodies used for analysis of the concentrated HIV-1 virions were: α-HIV-1 p24 monoclonal antibody (183-H12-5C) and antiserum to HIV-1 gp120 (DV-12) both from the NIH AIDS Reagent Program.

Subcellular Fractionation

A549 and HEK293 cells were infected with HA-Flag containing IAV PR8. To prepare

the crude ER extract homogenized cells were lysed in the buffer containing 1% Chaps, 50 mM Tris-HCl [pH 7.5], 150mM NaCl, 5 mM $MgCl_2$, protease inhibitor cocktail (Roche), phosphatase inhibitor (Sigma), and subjected to centrifugation (14,000 g, 15 min) to separate soluble ER fraction from nuclear fraction. The ER extract was layered for separation by ultracentrifugation on Optiprep (Sigma) discontinuous gradients prepared in the buffer containing 250mM Sucrose, 6 mM EDTA, 10 mMTris-HCl [pH 7.5].

Flow cytometry

For influenza studies, A549 cells were siRNA treated for 48 hours. Cells were infected at an MOI=0.8 for 7 hours. Cells were then fixed in 4% PFA in PBS. Cells were blocked in 5% BSA in PBS for 1hr on ice. Primary antibodies against HA trimers (6F12 (Tan et al., 2012) conjugated to AF-488), the M2 surface protein (E10, courtesy of Tom Moran), or MHC-I (BD #555554) were diluted in 5% BSA in PBS as appropriate and incubated for 1-2 hours on ice. Secondary antibodies Alexa-fluor-488 anti-mouse IgG were diluted 1:1000 in PBS/BSA and incubated with the M2 samples for 40 min on ice. Samples were thoroughly washed and data was collected on a BD FacsCalibur (Mount Sinai Shared Resource Core). Data was analyzed using FlowJo. For HIV-1 experiments 293T cells were transfected with HIV-1 R7.3 33A EGFP and HIV-1 LAI-GFP using 3 mg/ml polyethylenimine (Polysciences). Surface gp120 trimers were detected via staining with the human monoclonal antibody PG9 and Alexa-fluor-647 secondary antibody. Monomeric gp120 was detected using the human monoclonal antibody 2G12 and Alexa-fluor-647 as a secondary antibody. Dead cells were stained by LIVE/DEAD Fixable Aqua Dead Cell Stain (Life Technologies) and excluded from the analysis. Data were

collected on a BD™ LSR II flow cytometer and analyzed using FlowJo. In order to compare different antibodies, flow cytometry data are shown as fluorescent index where the mean fluorescent index of each point is multiplied by the percentage of double positive cells devoid of non specific background binding.

Glycosidase treatment and pulse-chase

A549 cells were infected at an MOI=1 for 1 hour. 7 hours post-infection, cell lysates (or immunoprecipitated HA) were treated with EndoH (NEB), PNGaseF (NEB), or buffer alone for 2 hours at 37C. Reactions were terminated by the addition of 2x Laemmli sample buffer. For pulse chase, A549 cells were infected as above. After 5 hours, cells were starved for Met and Cys for 30min. After starvation, cells were pulsed with EXPRE^{35}S^{35}S Protein Labeling Mix for 30 min. Labeling media was removed, and complete DMEM was added to chase for the indicated times. Total HA was immunoprecipitated with the PY102 antibody overnight at 4C. Immunoprecipitated HA was treated with EndoH, PNGase F, or buffer as described above. Labeled proteins were resolved via SDS-PAGE, gels were dried and exposed together on the same film at the same time for 18 hours.

Analysis of host factors controlling DENV replication

Knockdown of host factors was done using endonuclease-derived siRNAs (esiRNAs). esiRNAs targeting approximately 250nt of the target gene were designed using the DEQOR algorithm and synthesized as previously described (Roguev et al., 2013). For knockdown, 10ng of esiRNA were reverse transfected into Huh7 cells in 96-well format

with DharmaFECT4 (Thermo Fisher Scientific, T-2004-01) according to manufacturer protocols. Cells were infected with Renilla luciferase reporter virus (Samsa et al., 2009) at 72 hours post-transfection at an MOI of 0.1, and Renilla luciferase activity was measured 48 hours post-infection using the Renilla Luciferase Assay System (Promega, E2810) and a Veritas microplate luminometer according to manufacturer protocols. Knockdown was assessed by RT-qPCR using the CellAmp Direct RNA Prep kit (Takara, 3733), the SensiFAST One-Step RT-qPCR kit (Bioline, BIO-72001) and the BioRad CFX-96 thermocycler.

Generation of monocyte-derived dendritic cells (MDDCs)

Human MDDCs were obtained from healthy human blood donors (New York Blood Center), following a standard protocol. Briefly, after Ficoll-Hypaque gradient centrifugation, CD14+ cells were isolated from the mononuclear fraction using a MACS CD14 isolation kit (Milteny Biotec) according to the manufacturer's directions. CD14+ cells were then differentiated to naïve DCs by incubation during 5 to 6 days in DC medium (RPMI supplemented with 100 U/ml L-glutamine, 100 g/ml penicillin-streptomycin, and 1 mM sodium pyruvate) with the presence of 500 U/ml human granulocyte-macrophage colony-stimulated factor (GM-CSF) (PeproTech), 1,000 U/ml human interleukin 4 (IL-4) (PeproTech), and 10% FBS (Hyclone). The purity of the MDDCs was confirmed by flow cytometry analysis.

RNA isolation (DENV)

RNA from different cells was extracted using Quick RNATM MiniPrep (Zymo Research). The concentration was evaluated in a spectrophotometer at 260 nm, and 1000 ng of RNA were reverse transcribed using the iScript cDNA synthesis kit (Bio-Rad) according to the manufacturer's instructions.

qRT-PCR (DENV)

Evaluation of the expression of viral RNA was carried out using iQ SYBR green Supermix (Bio-Rad) according to the manufacturer's instructions. The PCR temperature profile was 95°C for 10 min, followed by 40 cycles of 95°C for 10 s and 60°C for 60 s. Expression levels for DENV RNA was calculated based on the CT values using rsp11 housekeeping gene to normalize the data.

DENV Viruses

Dengue virus serotype 2 (DENV-2) strains 16681 was used in this study. DENV was grown in C6/36 insect cells for 6 days. C6/36 cells were infected at an MOI=0.01, and 6 days after infection, cell supernatants were collected, clarified, and stored at 80°C. The titers of DENV stocks were determined by limiting-dilution plaque assay on BHK cells.

Cytotoxicity assay

In order to quantify the toxicity of MDDCs treated with CT8, The CytoTox 96® Non-Radioactive Cytotoxicity Assay (Promega) was used according to manufacturer's instructions. Briefly, MDDcs were incubated with either 100nM or 500nM of CT8 or same final % of DMSO in DC media and release of LDH was monitored for 24, 48, and

72 hpt. As positive control MDDCs were frozen and thawed 3 times at the specific times and supernatant was centrifuged at full speed.

Statistical analysis

Statistical analysis between datasets was performed using a two-tailed student's t-test. Differences were considered to be statistically significant at p-values at or below 0.05.

Supplemental References

Bindea, G., Mlecnik, B., Hackl, H., Charoentong, P., Tosolini, M., Kirilovsky, A., Fridman, W.H., Pages, F., Trajanoski, Z., and Galon, J. (2009). ClueGO: a Cytoscape plug-in to decipher functionally grouped gene ontology and pathway annotation networks. Bioinformatics *25*, 1091-1093.

Boussif, O., Lezoualch, F., Zanta, M.A., Mergny, M.D., Scherman, D., Demeneix, B., and Behr, J.P. (1995). A Versatile Vector for Gene and Oligonucleotide Transfer into Cells in Culture and in-Vivo - Polyethylenimine. Proceedings of the National Academy of Sciences of the United States of America *92*, 7297-7301.

Bradel-Tretheway, B.G., Mattiacio, J.L., Krasnoselsky, A., Stevenson, C., Purdy, D., Dewhurst, S., and Katze, M.G. (2011). Comprehensive Proteomic Analysis of Influenza Virus Polymerase Complex Reveals a Novel Association with Mitochondrial Proteins and RNA Polymerase Accessory Factors. Journal of virology *85*, 8569-8581.

Chakrabarti, L.A., Ivanovic, T., and Cheng-Mayer, C. (2002). Properties of the surface envelope glycoprotein associated with virulence of simian-human immunodeficiency virus SHIV(SF33A) molecular clones. Journal of virology *76*, 1588-1599.

Gentleman, R.C., Carey, V.J., Bates, D.M., Bolstad, B., Dettling, M., Dudoit, S., Ellis, B., Gautier, L., Ge, Y., Gentry, J.*, et al.* (2004). Bioconductor: open software development for computational biology and bioinformatics. Genome biology *5*, R80.

Jager, S., Cimermancic, P., Gulbahce, N., Johnson, J.R., McGovern, K.E., Clarke, S.C., Shales, M., Mercenne, G., Pache, L., Li, K.*, et al.* (2012). Global landscape of HIV-human protein complexes. Nature *481*, 365-370.

Jorba, N., Juarez, S., Torreira, E., Gastaminza, P., Zamarreno, N., Albar, J.P., and Ortin, J. (2008). Analysis of the interaction of influenza virus polymerase complex with human cell factors. Proteomics *8*, 2077-2088.

Lin, L., Li, Y., Pyo, H.M., Lu, X.Y., Raman, S.N.T., Liu, Q., Brown, E.G., and Zhou, Y. (2012). Identification of RNA Helicase A as a Cellular Factor That Interacts with Influenza A Virus NS1 Protein and Its Role in the Virus Life Cycle. Journal of virology *86*, 1942-1954.

Lue, J., Hsu, M., Yang, D., Marx, P., Chen, Z.W., and Cheng-Mayer, C. (2002). Addition of a single gp120 glycan confers increased binding to dendritic cell-specific ICAM-3-grabbing nonintegrin and neutralization escape to human immunodeficiency virus type 1. Journal of virology *76*, 10299-10306.

Mayer, D., Molawi, K., Martinez-Sobrido, L., Ghanem, A., Thomas, S., Baginsky, S., Grossmann, J., Garcia-Sastre, A., and Schwemmle, M. (2007). Identification of cellular interaction partners of the influenza virus ribonucleoprotein complex and polymerase complex using proteomic-based approaches. Journal of proteome research *6*, 672-682.

Mellacheruvu, D., Wright, Z., Couzens, A.L., Lambert, J.P., St-Denis, N.A., Li, T., Miteva, Y.V., Hauri, S., Sardiu, M.E., Low, T.Y.*, et al.* (2013). The CRAPome: a contaminant repository for affinity purification-mass spectrometry data. Nature methods *10*, 730-736.

Menche, J., Sharma, A., Kitsak, M., Ghiassian, S.D., Vidal, M., Loscalzo, J., and Barabasi, A.L. (2015). Disease networks. Uncovering disease-disease relationships through the incomplete interactome. Science *347*, 1257601.

Miller, M.S., Rialdi, A., Ho, J.S., Tilove, M., Martinez-Gil, L., Moshkina, N.P., Peralta, Z., Noel, J., Melegari, C., Maestre, A.M.*, et al.* (2015). Senataxin suppresses the antiviral transcriptional response and controls viral biogenesis. Nat Immunol *16*, 485-494.

Moran, T., Liu, Y.N.C., Schulman, J.L., and Bona, C.A. (1984). Shared Idiotopes among Monoclonal-Antibodies Specific for a/Pr/8/34 (H1n1) and X-31(H3n2) Influenza-Viruses. P Natl Acad Sci-Biol *81*, 1809-1812.

Navratil, V., de Chassey, B., Meyniel, L., Delmotte, S., Gautier, C., Andre, P., Lotteau, V., and Rabourdin-Combe, C. (2009). VirHostNet: a knowledge base for the management and the analysis of proteome-wide virus-host interaction networks. Nucleic acids research *37*, D661-668.

Reimand, J., Arak, T., and Vilo, J. (2011). g:Profiler--a web server for functional interpretation of gene lists (2011 update). Nucleic acids research *39*, W307-315.

Roguev, A., Talbot, D., Negri, G.L., Shales, M., Cagney, G., Bandyopadhyay, S., Panning, B., and Krogan, N.J. (2013). Quantitative genetic-interaction mapping in mammalian cells. Nature methods *10*, 432-437.

Samsa, M.M., Mondotte, J.A., Iglesias, N.G., Assuncao-Miranda, I., Barbosa-Lima, G., Da Poian, A.T., Bozza, P.T., and Gamarnik, A.V. (2009). Dengue virus capsid protein usurps lipid droplets for viral particle formation. Plos Pathog *5*, e1000632.

Shaw, M.L., Stone, K.L., Colangelo, C.M., Gulcicek, E.E., and Palese, P. (2008). Cellular proteins in influenza virus particles. Plos Pathog *4*, e1000085.

Smoot, M.E., Ono, K., Ruscheinski, J., Wang, P.L., and Ideker, T. (2011). Cytoscape 2.8: new features for data integration and network visualization. Bioinformatics *27*, 431-432.

Tafforeau, L., Chantier, T., Pradezynski, F., Pellet, J., Mangeot, P.E., Vidalain, P.O., Andre, P., Rabourdin-Combe, C., and Lotteau, V. (2011). Generation and comprehensive analysis of an influenza virus polymerase cellular interaction network. Journal of virology *85*, 13010-13018.

Tan, G.S., Krammer, F., Eggink, D., Kongchanagul, A., Moran, T.M., and Palese, P. (2012). A pan-H1 anti-hemagglutinin monoclonal antibody with potent broad-spectrum efficacy in vivo. Journal of virology *86*, 6179-6188.

Watanabe, T., Kawakami, E., Shoemaker, J.E., Lopes, T.J., Matsuoka, Y., Tomita, Y., Kozuka-Hata, H., Gorai, T., Kuwahara, T., Takeda, E.*, et al.* (2014). Influenza virus-host interactome screen as a platform for antiviral drug development. Cell host & microbe *16*, 795-805.

Watanabe, T., Watanabe, S., and Kawaoka, Y. (2010). Cellular networks involved in the influenza virus life cycle. Cell host & microbe *7*, 427-439.

Wiertz, E.J., Tortorella, D., Bogyo, M., Yu, J., Mothes, W., Jones, T.R., Rapoport, T.A., and Ploegh, H.L. (1996). Sec61-mediated transfer of a membrane protein from the endoplasmic reticulum to the proteasome for destruction. Nature *384*, 432-438.